

Dielectrophoretic Assembly of Gold Nanoparticle Arrays Evaluated in Terms of Room-Temperature Resistance

著者 (英)	Yoshinao MIZUGAKI, Makoto MORIBAYASHI, Tomoki YAGAI, Masataka MORIYA, Hiroshi SHIMADA, Ayumi HIRANO-IWATA, Fumihiko HIROSE
journal or publication title	IEICE Transactions on Electronics
volume	E103.C
number	2
page range	62-65
year	2020-02-01
URL	http://id.nii.ac.jp/1438/00009634/

doi: 10.1587/transele.2019ECS6011

BRIEF PAPER

Dielectrophoretic Assembly of Gold Nanoparticle Arrays Evaluated in Terms of Room-Temperature Resistance

Yoshinao MIZUGAKI^{†a)}, *Member*, Makoto MORIBAYASHI[†], Tomoki YAGAI[†], *Nonmembers*, Masataka MORIYA[†], *Member*, Hiroshi SHIMADA[†], Ayumi HIRANO-IWATA^{††}, *Nonmembers*, and Fumihiko HIROSE^{†††}, *Member*

SUMMARY Gold nanoparticles (GNPs) are often used as island electrodes of single-electron (SE) devices. One of technical challenges in fabrication of SE devices with GNPs is the placement of GNPs in a nanogap between two lead electrodes. Utilization of dielectrophoresis (DEP) phenomena is one of possible solutions for this challenge, whereas the fabrication process with DEP includes stochastic aspects. In this brief paper, we present our experimental results on electric resistance of GNP arrays assembled by DEP. More than 300 pairs of electrodes were investigated under various DEP conditions by trial and error approach. We evaluated the relationship between the DEP conditions and the electric resistance of assembled GNP arrays, which would indicate possible DEP conditions for fabrication of SE devices.

key words: single-electron effect, Coulomb blockade, histogram, tunnel junction

1. Introduction

Single-electron (SE) devices [1], which are one of the candidates for the “beyond CMOS” technologies [2], are composed of several tiny tunnel junctions and tiny island electrodes. Since the report by Schönberger *et al.* [3], gold nanoparticles (GNPs) have been often used for island electrodes in SE devices because of their small sizes and chemical stability. In regard to lead electrodes, besides a tip of a scanning probe microscope, two metal electrodes placed across a nanogap are commonly used for the source and drain electrodes [4]–[8]. For such a pair of two electrodes, it is a technical challenge to embed one or a few GNPs in the nanogap.

Utilization of dielectrophoresis (DEP) phenomena is one of the techniques to convey GNPs into a nanogap [9]–[16]. A non-uniform electric field exerts a dielectrophoretic force on a dielectric particle in the field. The time-averaged DEP force $\langle F_{\text{DEP}}(t) \rangle$ is expressed as

$$\langle F_{\text{DEP}}(t) \rangle = 2\pi\epsilon_m a^3 \text{Re}[K(\omega)] \nabla |E_{\text{rms}}|^2 \quad (1)$$

where ϵ_m , a , $K(\omega)$, and E_{rms} are the permittivity of the medium, the radius of the nanoparticle, the Clausius-

Manuscript received April 23, 2019.

Manuscript revised June 27, 2019.

Manuscript publicized August 5, 2019.

[†]The authors are with The University of Electro-Communications, Chofu-shi, 182–8585 Japan.

^{††}The author is with Tohoku University, Sendai-shi, 980–8577 Japan.

^{†††}The author is with Yamagata University, Yonezawa-shi, 992–8510 Japan.

a) E-mail: y.mizugaki@uec.ac.jp

DOI: 10.1587/transele.2019ECS6011

Mossotti factor, and the rms value of the electric field, respectively [17].

So far, several groups have reported SE devices in which GNPs are assembled in an electrode gap by using the DEP force [18]–[20]. Parameters related to DEP, such as the voltages, frequencies, layouts of electrodes, etc., have been also investigated [17], [22], [23].

We have also tried to fabricate SE devices using DEP [21]. Some devices exhibited clear characteristics of the Coulomb blockade and Coulomb oscillation. On the other hand, we have found that a wide variety of GNP arrays are realized under the nearly same DEP conditions. It is no wonder that we do not obtain the identical arrays made of a small number of GNPs since the microscopic DEP conditions are not static. For example, the positions of all GNPs in a colloidal solution are changing at every moment. GNPs attached on the electrodes simultaneously change the electric field around the gap. That is, from the viewpoint of SE devices, the fabrication process utilizing the DEP force includes stochastic aspects.

In this brief paper, we present our experimental results on electric resistance of GNP arrays assembled by DEP. Although the electric resistance of GNP array was measured at room temperature, it was good predictor of electric properties at low temperature. More than 300 pairs of electrodes were investigated under various DEP conditions by trial and error approach. Although the experimental conditions were not strictly systematized, we evaluated the relationship between the DEP conditions and the electric resistance of GNP arrays, which would indicate possible DEP conditions for fabrication of SE devices.

2. Experiments

Samples were prepared as follows. First, NiCr/Au electrodes were made on a Si/SiO₂ substrate by using e-beam lithography and a shadow evaporation technique. The thicknesses of the first and second evaporation of NiCr/Au layers were 5/20 and 5/45 nm, respectively. The layout of electrodes is illustrated in Fig. 1. Typically, 7 pairs of electrodes were fabricated on a sample. A part of samples were immersed in a 5 mM ethanol solution of either 1,10-decanedithiol or 1,4-butanedithiol for 18 hours at room temperature, which resulted in SAM coating on the electrodes.

Next, the DEP process with a colloidal citric solution of GNPs was conducted. The diameter and density of GNPs

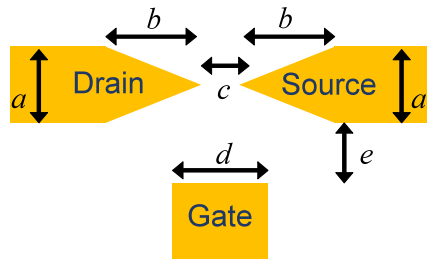


Fig. 1 Schematic illustration of electrodes (top view). An AC voltage was applied between the source and drain electrode. The dimensions are as follows. a : 800 nm, b : $1.2\ \mu\text{m}$, c : 100–200 nm as the target value (actually fabricated in the range of 100–400 nm), d : 500–900 nm, e : 0– $1\ \mu\text{m}$.

were $30\ \text{nm}$ and $1.8 \times 10^{11}/\text{mL}$, respectively. For some experiments, the surface of GNPs were modified by mixing the GNP colloidal solution and a 0.1 mM ethanol solution of 1-decanethiol with the volume ratio of $400\ \mu\text{L}$ and $200\ \mu\text{L}$. After dropping $10\ \mu\text{L}$ of gold colloidal solution on a sample, an AC sinusoidal voltage of $1\text{--}10\ \text{V}_{\text{p-p}}$ (V_{DEP}) and $100\ \text{Hz}\text{--}10\ \text{MHz}$ (f_{DEP}) was applied across two electrodes (source and drain) for $2\ \text{s}\text{--}10\ \text{min}$ (T_{DEP}). The voltage waveform was monitored on an oscilloscope. It should be noted that we conducted the DEP process one by one for all electrode pairs on the sample with one drop of GNP colloidal solution. Because of solvent evaporation, the GNP density was not kept constant during the DEP processes even on the same sample. After the DEP process, the sample was rinsed in pure water and then dried with N_2 gas blow.

GNP arrays were evaluated by three methods, SEM observation, electric resistance measurement at room temperature, and measurement of $I\text{--}V$ characteristics at low temperature.

We observed all electrode pairs by using an FE-SEM. From SEM images in a $500 \times 500\ \text{nm}^2$ region near the electrode gap, we extracted the area occupied by GNPs. This GNP area (S_{GNP}) is an evaluation index of GNPs assembled by the DEP process.

Then, at room temperature, the resistance values of all electrode pairs were measured by a resistance meter with self-build terminals. The effective measuring range was between $10\ \text{k}\Omega$ and $28\ \text{G}\Omega$. It was empirically observed in our preceding experiments that the electrode pairs having the resistance values out of this range seldom exhibited the Coulomb blockade. Thus, the room-temperature resistance (R_{RT}) is another evaluation index.

Finally, $I\text{--}V$ characteristics were measured in a liquid helium bath. Due to the experimental costs, 25 electrode pairs were evaluated.

3. Results and Discussion

Figure 2 shows an example of the SE devices fabricated using the DEP process, where surface-modified electrodes were used with the DEP conditions of $f_{\text{DEP}} = 1000\ \text{kHz}$, $V_{\text{DEP}} = 4\ \text{V}$, and $T_{\text{DEP}} = 10\ \text{s}$. It is found in Fig. 2(a) that GNPs are assembled in the electrode gap. S_{GNP} was

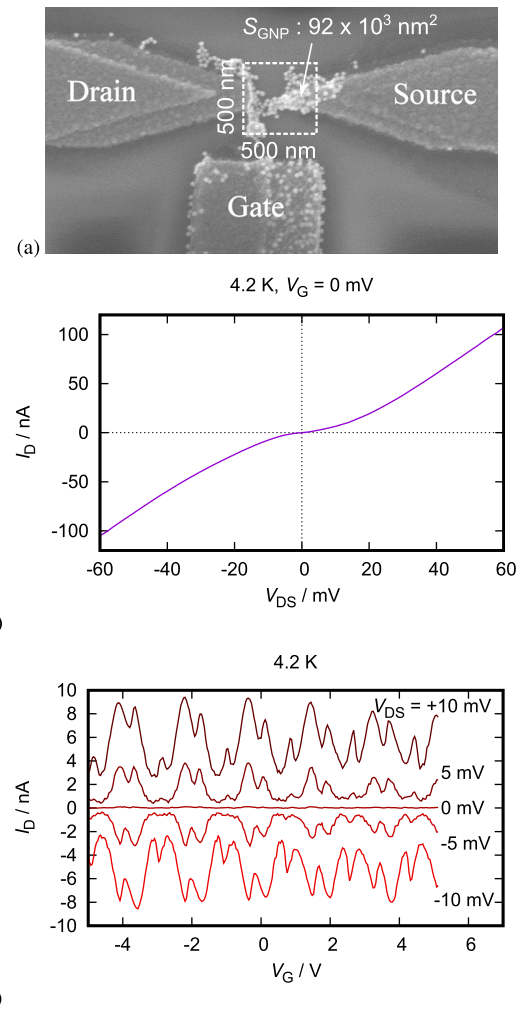


Fig. 2 Example of the fabricated devices ($f_{\text{DEP}} = 1000\ \text{kHz}$, $V_{\text{DEP}} = 4\ \text{V}$, $T_{\text{DEP}} = 10\ \text{s}$). (a) SEM image around the electrode gap. S_{GNP} and R_{RT} are $92 \times 10^3\ \text{nm}^2$ and $360\ \text{k}\Omega$, respectively. (b) Drain current (I_{D}) vs. drain-source voltage (V_{DS}) characteristics at 4.2 K (c) I_{D} vs. gate voltage (V_{G}) characteristics at 4.2 K.

determined to be $92 \times 10^3\ \text{nm}^2$, whereas R_{RT} was $360\ \text{k}\Omega$. Electric properties at liquid helium temperature shown in Figs. 2(b) and 2(c) demonstrate clear Coulomb blockade and Coulomb oscillation.

As described in the introduction, the DEP process is rather stochastic. In other words, while we succeeded to fabricate SE devices as shown in Fig. 2, we also had electrode pairs that exhibited electric characteristics like a linear resistor or an insulator. To find out better DEP conditions for fabrication of SE devices, we employ not rigorous but somewhat statistical approach. R_{RT} is used for the main index. It is noted again that electrode pairs having R_{RT} between $10\ \text{k}\Omega$ and $28\ \text{G}\Omega$, which is hereafter referred to as the intermediate R_{RT} , are empirically expected to work as SE devices. The numbers of electrode pairs classified by R_{RT} and the electric characteristics measured at 4.2 K are tabulated in Table 1, which supports our empirical assumption.

The first analysis is the f_{DEP} dependence of R_{RT} shown

Table 1 Number of electrode pairs classified by R_{RT} and the electric characteristics measured at 4.2 K.

R_{RT}	Electric properties at 4.2 K		
	linear	non-linear	open
$< 10 \text{ k}\Omega$	1	0	0
$10 \text{ k}\Omega - 28 \text{ G}\Omega$	0	13	0
$> 28 \text{ G}\Omega$	0	2	9

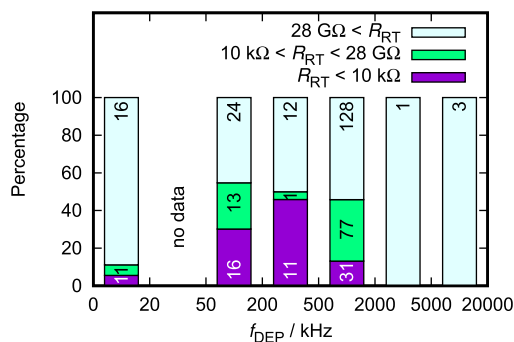


Fig. 3 R_{RT} distribution classified by f_{DEP} . Numerals in bins represent the number of corresponding electrode pairs. Note that the f_{DEP} regions on the horizontal axis are not equally divided.

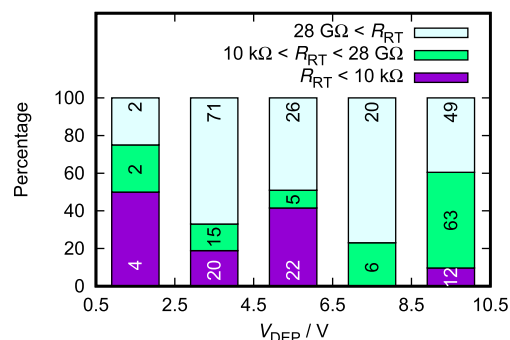


Fig. 4 R_{RT} distribution classified by V_{DEP} for $f_{DEP} > 20 \text{ kHz}$. Numerals in bins represent the number of corresponding electrode pairs.

in Fig. 3, where all results for the fabrication conditions described in the previous section are included. It is found that the intermediate R_{RT} is obtained for $50 < f_{DEP} < 2000 \text{ kHz}$. For $f_{DEP} < 20 \text{ kHz}$, 16 among 18 samples have R_{RT} larger than $28 \text{ G}\Omega$, which allow us to exclude the results for $f_{DEP} < 20 \text{ kHz}$ hereafter. On the other hand, although we obtained no samples having the intermediate R_{RT} for $f_{DEP} > 2000 \text{ kHz}$, we include them for the further analyses because the number of samples are too small to exclude them.

Next, dependence analyses of R_{RT} on V_{DEP} , T_{DEP} and the product of $T_{DEP}V_{DEP}$ are respectively presented in Figs. 4, 5, and 6. It is seen that the intermediate R_{RT} is efficiently obtained under the DEP conditions of $V_{DEP} > 8.5 \text{ V}$, $T_{DEP} > 50 \text{ s}$, and $T_{DEP}V_{DEP} > 200 \text{ Vs}$. The upper limits for these parameters cannot be determined due to the limited number of samples.

Finally, relationship between R_{RT} and S_{GNP} is presented in Fig. 7. It is found that larger S_{GNP} is effective to make R_{RT}

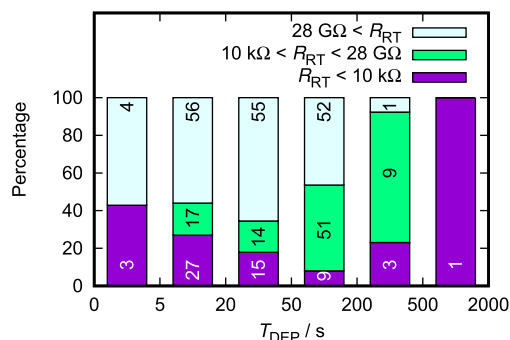


Fig. 5 R_{RT} distribution classified by T_{DEP} for $f_{DEP} > 20 \text{ kHz}$. Numerals in bins represent the number of corresponding electrode pairs. Note that the T_{DEP} regions on the horizontal axis are not equally divided.

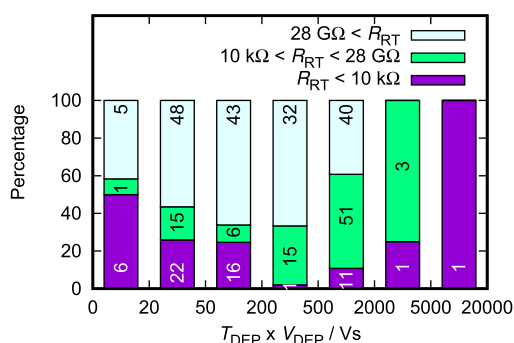


Fig. 6 R_{RT} distribution classified by the product of T_{DEP} and V_{DEP} for $f_{DEP} > 20 \text{ kHz}$. Numerals in bins represent the number of corresponding electrode pairs. Note that the $T_{DEP}V_{DEP}$ regions on the horizontal axis are not equally divided.

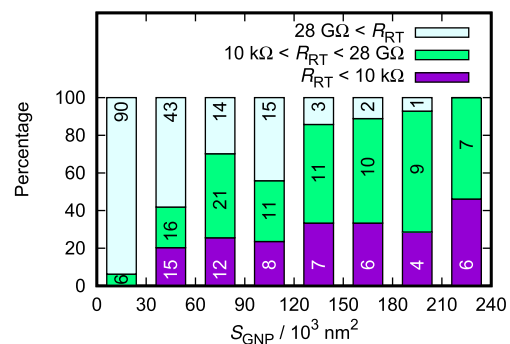


Fig. 7 R_{RT} distribution classified by S_{GNP} for $f_{DEP} > 20 \text{ kHz}$. Numerals in bins represent the number of corresponding electrode pairs.

smaller than $28 \text{ G}\Omega$. A threshold exists near $30 \times 10^3 \text{ nm}^2$, above which electrode pairs have finite resistance. Another threshold seems to be near $120 \times 10^3 \text{ nm}^2$, above which insulative states almost disappear. Such S_{GNP} dependence of R_{RT} agrees with the natural relationship between the electrical connection and the amount of assembled GNPs.

4. Conclusion

We presented our experimental results on electric resistance of GNP arrays assembled by DEP. More than 300 pairs

of electrodes were investigated under various DEP conditions by trial and error approach. We evaluated the relationship between the DEP conditions and the electric resistance of GNP arrays, which would suggest possible DEP conditions for fabrication of SE devices. That is, the conditions of $f_{\text{DEP}} > 20$ kHz, $V_{\text{DEP}} > 8.5$ V, $T_{\text{DEP}} > 50$ s, and $T_{\text{DEP}} V_{\text{DEP}} > 200$ Vs provide rough guidelines.

The results presented above were obtained in our experiments by trial and error. For further statistical evaluation of the DEP process, experiments should be organized well. However, although they included trivial conclusions, these results are the first step for combining the DEP conditions and electric characteristics of GNP arrays.

Acknowledgments

This work was partly supported by JSPS KAKENHI Grant Number 17K04979, and by JST-CREST Grant Number JP-MJCR14F. The authors are grateful to other lab. members in UEC Tokyo for fruitful discussion and technical supports. Nation-wide Cooperative Research Projects, Research Institute of Electrical Communication, Tohoku University are also acknowledged.

References

- [1] K.K. Likharev, "Single-electron devices and their applications," *Proc. IEEE*, vol.87, no.4, pp.606–632, 1999. DOI: 10.1109/5.752518
- [2] J.A. Hutchby, G.I. Bourianoff, V.V. Zhirnov, and J.E. Brewer, "Extending the road beyond CMOS," *IEEE Circuits Devices Mag.*, vol.18, no.2, pp.28–41, March, 2002. DOI: 10.1109/101.994856
- [3] C. Schönenberger, H. van Houten, and H.C. Donkersloot, "Single-electron tunnelling observed at room temperature by scanning-tunnelling microscopy," *Europhys. Lett.*, vol.20, no.3, pp.249–254, Oct. 1992. DOI: 10.1209/0295-5075/20/3/010
- [4] T. Sato, H. Ahmed, D. Brown, and B.F.G. Johnson, "Single electron transistor using a molecularly linked gold colloidal particle chain," *J. Appl. Phys.*, vol.82, no.2, pp.696–701, July 1997. DOI: 10.1063/1.365600
- [5] N. Okabayashi, K. Maeda, T. Muraki, D. Tanaka, M. Sakamoto, T. Teranishi, and Y. Majima, "Uniform charging energy of single-electron transistors by using size-controlled Au nanoparticles," *Appl. Phys. Lett.*, vol.100, no.3, 033101, Jan. 2012. DOI: 10.1063/1.3676191
- [6] H.T.T. Tran, K. Matsumoto, M. Moriya, H. Shimada, Y. Kimura, A. Hirano-Iwata, and Y. Mizugaki, "Fabrication of high temperature capacitively- and resistively-coupled single electron transistors using gold nanoparticles," *Proc. 16th Int. Conf. Nanotechnology (IEEE NANO 2016)*, Sendai, Japan, TuPo1.20, pp.131–134, Aug. 2016. DOI: 10.1109/NANO.2016.7751353
- [7] T.T.T. Huong, K. Matsumoto, M. Moriya, H. Shimada, Y. Kimura, A. Hirano-Iwata, and Y. Mizugaki, "Gate-tuned negative differential resistance observed at room temperature in an array of gold nanoparticles," *Appl. Phys. A*, vol.123, no.4, 268, April 2017. DOI: 10.1007/s00339-017-0891-8
- [8] Y. Mizugaki, K. Matsumoto, M. Moriya, H. Shimada, A. Hirano-Iwata, and F. Hirose, "One-dimensional array of small tunnel junctions fabricated using 30-nm-diameter gold nanoparticles placed in a 140-nm-wide resist groove," *Jpn. J. Appl. Phys.*, vol.57, no.9, 098006, Sept. 2018. DOI: 10.7567/JJAP.57.098006
- [9] I. Amlani, A.M. Rawlett, L.A. Nagahara, and R.K. Tsui, "An approach to transport measurements of electronic molecules," *Appl. Phys. Lett.*, vol.80, no.15, pp.2761–2763, April 2002. DOI: 10.1063/1.1469655
- [10] L. Zheng, S. Li, J.P. Brody, and P.J. Burke, "Manipulating nanoparticles in solution with electrically contacted nanotubes using dielectrophoresis," *Langmuir*, vol.20, no.20, pp.8612–8619, Sept. 2004. DOI: 10.1021/la049687h
- [11] S.O. Lumsdon and D.M. Scott, "Assembly of colloidal particles into microwires using an alternating electric field," *Langmuir*, vol.21, no.11, pp.4874–4880, May 2005. DOI: 10.1021/la0472697
- [12] R.J. Barsotti Jr., M.D. Vahey, R. Wartena, Y.-M. Chiang, J. Voldman, and F. Stellacci, "Assembly of Metal Nanoparticles into Nanogaps," *Small*, vol.3, no.3, pp.488–499, March 2007. DOI: 10.1002/sml.200600334
- [13] S. Kumar, Y.-K. Seo, and G.-H. Kim, "Manipulation and trapping of semiconducting ZnO nanoparticles into nanogap electrodes by dielectrophoresis technique," *Appl. Phys. Lett.*, vol.94, no.15, 153104, April 2009. DOI: 10.1063/1.3118588
- [14] D. Cheon, S. Kumar, and G.-H. Kim, "Assembly of gold nanoparticles of different diameters between nanogap electrodes," *Appl. Phys. Lett.*, vol.96, no.1, 013101, Jan. 2010. DOI: 10.1063/1.3280859
- [15] W. Liu, C. Wang, H. Ding, J. Shao, and Y. Ding, "AC electric field induced dielectrophoretic assembly behavior of gold nanoparticles in a wide frequency range," *Appl. Surf. Sci.*, vol.370, pp.184–192, May 2016. DOI: 10.1016/j.apsusc.2016.02.118
- [16] A. Barik, X. Chen, and S.-H. Oh, "Ultralow-power electronic trapping of nanoparticles with sub-10 nm gold nanogap electrodes," *Nano Lett.*, vol.16, no.10, pp.6317–6324, Oct., 2016. DOI: 10.1021/acs.nanolett.6b02690
- [17] B.C. Gierhart, D.G. Howitt, S.J. Chen, R.L. Smith, and S.D. Collins, "Frequency dependence of gold nanoparticle superassembly by dielectrophoresis," *Langmuir*, vol.23, no.24, pp.12450–12456, Nov. 2007. DOI: 10.1021/la701472y
- [18] S.H. Hong, H.K. Kim, K.H. Cho, S.W. Hwang, J.S. Hwang, and D. Ahn, "Fabrication of single electron transistors with molecular tunnel barriers using ac dielectrophoresis technique," *J. Vac. Sci. Technol. B*, vol.24, no.1, pp.136–138, Jan. 2006. DOI: 10.1116/1.2150227
- [19] S.I. Khondaker, K. Luo, and Z. Yao, "The fabrication of single-electron transistors using dielectrophoretic trapping of individual gold nanoparticles," *Nanotechnology*, vol.21, no.9, 095204, March 2010. DOI: 10.1088/0957-4484/21/9/095204
- [20] S.K. Bose, C.P. Lawrence, Z. Liu, K.S. Makarenko, R.M.J. van Damme, H.J. Broersma, and W.G. van der Wiel, "Evolution of a designless nanoparticle network into reconfigurable Boolean logic," *Nat. Nanotech.*, vol.10, pp.1048–1052, Dec. 2015. DOI: 10.1038/NNANO.2015.207
- [21] M. Moribayashi, T. Yagai, M. Moriya, H. Shimada, A. Hirano-Iwata, F. Hirose, and Y. Mizugaki, "Single-electron charging effects observed in arrays of gold nanoparticles formed by dielectrophoresis between SAM-coated electrodes," *AIP Conf. Proc.*, vol.2067, 020019, Jan. 2019. DOI: 10.1063/1.5089452
- [22] H. Ding, W. Liu, J. Shao, Y. Ding, L. Zhang, and J. Niu, "Influence of induced-charge electrokinetic phenomena on the dielectrophoretic assembly of gold nanoparticles in a conductive-island-based microelectrode system," *Langmuir*, vol.29, no.39, pp.12093–12103, Oct. 2013. DOI: 10.1021/la402060g
- [23] T. Koshi and E. Iwase, "Self-healing metal wire using electric field trapping of metal nanoparticles," *Jpn. J. Appl. Phys.*, vol.54, no.6S1, 06FP03, June 2015. DOI: 10.7567/JJAP.54.06FP03